(9) ten Brinke, G.; Ausserre, D.; Hadziioannou, G. *J. Chem. Phys.* **1988**, *89*, 4374.
(10) Kumar, S. K.; Vacatello, M.; Yoon, D. Y. *J. Chem. Phys.* **1988**, *89*, 5206.
(11) Scheutjens, J. M. H. M.; Fleer, G. J. *J. Phys. Chem.* **1979**, *83*, 1619.
(12) Scheutjens, J. M. H. M.; Fleer, G. J. *Macromolecules* **1985**, *18*, 1882.
(13) Weibull, W. J. *Appl. Mech.* **1951**, *18*, 293.
(14) Rosenbluth, M. N.; Rosenbluth, A. W. *J. Chem. Phys.* **1955**, *23*, 356.
(15) Verdier, P. H.; Stockmayer, W. H. *J. Chem. Phys.* **1962**, *36*, 227.
(16) Wall, F. T.; Mandel, F. *J. Chem. Phys.* **1975**, *63*, 4592.
(17) For a review, see ref 2 and the references therein.

Stiffness of Oriented Flexible-Chain Polymers

Aaldrik R. Postema[†,‡] and Paul Smith[*,‡,§]

Materials Department and Department of Chemical & Nuclear Engineering, University of California at Santa Barbara, Santa Barbara, California 93106

Received September 25, 1989; Revised Manuscript Received January 29, 1990

ABSTRACT: The stiffness of oriented, flexible-chain polymers is discussed. This paper elaborates on a previously introduced theory for the development of the axial Young's modulus with the draw ratio of flexible macromolecules. Here, the model is applied to uniaxially oriented poly(ethylene terephthalate), poly(oxymethylene), isotactic polypropylene, and poly(*p*-xylylene). Special attention is devoted to the prediction of the limits, set by the molecular weight, to the maximum Young's modulus that can be achieved through tensile drawing.

Introduction

In a previous paper[1] a simple theory was presented for the development of the axial Young's modulus with a draw ratio of flexible-chain molecules. The model is based on the assumption that orientational drawing of flexible polymers proceeds in an affine fashion; its applicability is therefore limited to experimental conditions favoring affine deformation, such as relatively low drawing temperatures. In the model, the partially oriented polymer is considered to be comprised of only two types of elastic elements; "helix" elements, which are perfectly oriented in the direction of the draw, and "coil" elements, which are unoriented. Tensile drawing is understood to increase the fraction, f_h, of helix elements at the expense of the fraction of coil elements, $1 - f_h$. The two elements are characterized by their respective moduli: E_h, the theoretical axial chain modulus, and E_u, the modulus of the unoriented material in which, strictly speaking, $f_h = 0$. The rationale for this simple two-state approach, which was previously employed by Hermans[2] and Fraser,[3] finds its origin in the recognition that the stiffness of most oriented polymers is extremely anisotropic and that the off-axis modulus is essentially independent of the test direction over a wide range of angles (Ward[4] and Bastiaansen et al.[5]).

Following Ward et al.,[6] the model assumes a uniform stress distribution in the helix and coil elements. On the basis of these assumptions, the Young's modulus of a flexible polymer that is drawn to a draw ratio, λ, is given[1] by the equation

$$E = \left(E_u^{-1} - \left[\frac{3\lambda^3}{2(\lambda^3 - 1)} [1 - (\lambda^3 - 1)^{-1/2} \tan^{-1} \{(\lambda^3 - 1)^{1/2}\}] - \frac{1}{2} \right] (E_u^{-1} - E_h^{-1}) \right)^{-1} \quad (1)$$

which for $\lambda \geq 5$ to good approximation reduces to

$$E = \left[E_h^{-1} + (E_u^{-1} - E_h^{-1}) \left(\frac{3\pi}{4}\right) \lambda^{-3/2} \right]^{-1} \quad (2)$$

It is of interest to note that a plot of E^{-1} vs $\lambda^{-3/2}$, at sufficiently high values of λ, is predicted to yield a straight line with slope $(E_u^{-1} - E_h^{-1})(3\pi/4)$ and an intercept at $\lambda^{-3/2} = 0$ of E_h^{-1} (the reciprocal theoretical modulus). This implies that the model is particularly well-suited to predict theoretical axial moduli of flexible-chain polymers.

Equations 1 and 2 do not contain any molecular weight dependent variables or parameters. Thus the model predicts, in agreement with numerous experimental observations, that the Young's modulus depends uniquely on the absolute draw ratio, provided that deformation proceeded in a (near) affine mode. The molecular weight, or rather chain length, does set an upper limit, however, to the average maximum ratio, $\lambda_{max,net}$, to which a molecular network can be elongated.[7,8] The latter quantity to a good approximation (for values of $\lambda > 2$) is given by

$$\lambda_{max,net} = (3)^{1/2}(l_p/l)(n/C_\infty)^{1/2} \quad (3)$$

Here n is the number of chain segments, having a length l and a projected length l_p in the chain direction and C_∞ is the characteristic ratio.[7,9] (The prefactor $(3)^{1/2}$, which was not considered in ref 1, stems from network considerations.[8]) This maximum draw ratio directly trans-

† Present address: ICI Europa Ltd., Everslaan 45, B-3078 Kortenberg, Belgium.
‡ Materials Department.
§ Department of Chemical & Nuclear Engineering.

0024-9297/90/2223-3296$02.50/0

Table I
Characteristic Ratios (C_∞), Lengths (l), Projected Lengths (l_p), and Masses of Chain Segments

polymer	C_∞	l, nm	l_p, nm	M, kg/kmol
poly(ethylene terephthalate)[10]	4.2	0.214	0.179	32.03
poly(oxymethylene)[11]	7.5	0.143	0.096	15.01
isotactic polypropylene[12]	5.7	0.153	0.110	21.04

lates, of course, into a *molecular weight dependent* upper limit to the Young's modulus that can be achieved through tensile drawing. The latter value can be calculated from relation 1 or 2 and eq 3. A matter of uncertainty arises in the latter operation when systems composed of chains of various lengths are dealt with. A priori, it is not obvious which moment of the chain length distribution should be employed in the calculation of $\lambda_{max,net}$ and whether or not the choice of the particular moment is affected by the nature of the distribution. The argument can be put forth that a network of heterodisperse chain molecules is bound to fail when a significant fraction of the macromolecules is elongated to their maximum draw ratio and that the number-averaged chain length should be substituted in relation.[3] On the other hand, in ref 1, we made the observation that excellent agreement was found between the predicted maximum modulus and the reported experimental values when they were plotted against the weight average molecular weight of the samples used, and the prefactor $(3)^{1/2}$ was omitted, i.e., when we used the relation

$$\lambda_{max,net} = (l_p/l)(n_w/C_\infty)^{1/2} \qquad (3')$$

Thus, both methods of computation will be adopted in this work. Further discussion of this important issue and of the experimental factors that may prevent realization of the maximum draw ratios is deferred to the final section of this paper.

Confidence in the validity of the rather simple theory, which, unlike other models, is free from cumbersome detailed morphological information, was derived from excellent agreement between the calculated and experimental moduli versus the draw ratio for linear polyethylenes.[1] In the present paper we extend its application to other flexible-chain polymers—poly(ethylene terephthalate), isotactic polypropylene, poly(oxymethylene), and poly(*p*-xylylene)—that are oriented through tensile drawing. The experimental data used in this work were retrieved from the literature. It was ensured that the modulus data selected were collected under comparable conditions.

Results

In the following section, modulus/draw ratio data of four different, mostly commercially important, polymers will be analyzed and contrasted against theoretical predictions. The various parameters needed in the calculation of maximum draw ratios for different molecular weights (eq 3) are given in Table I.

Poly(ethylene terephthalate). Experimental values of the room-temperature Young's modulus as a function of the draw ratio of oriented poly(ethylene terephthalate) (PET) have been published, among many others, by Pinnock and Ward[13] and Pereira and Porter.[14] The samples used by Pinnock and Ward[13] were prepared in a two-stage melt-spinning and drawing process. Drawing of the melt-spun PET fibers was carried out in two different ways: "pin-only", where the fibers were passed over a heated cylindrical pin, and "pin-and-plate" drawing, in which the fibers were passed over the heated pin and, subsequently, over a heated plate. The samples of Pereira and Porter[14] were prepared by solid-state coextrusion.

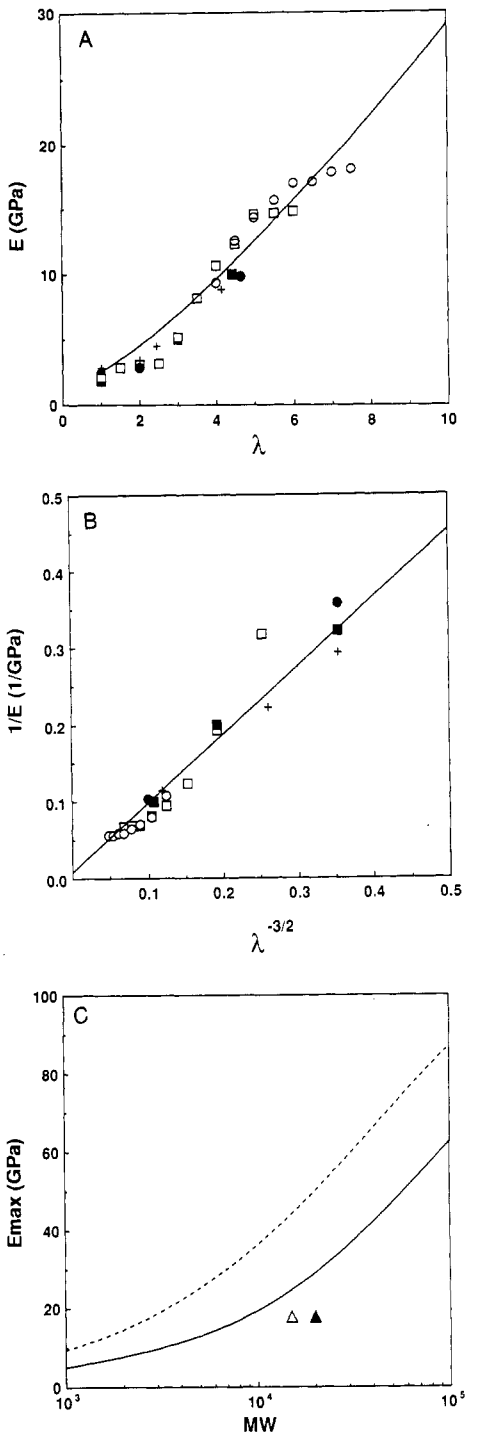

Figure 1. (A) Experimental data of the axial Young's modulus E versus the draw ratio, λ, of poly(ethylene terephthalate). Solid line calculated with eq 1 (E_h = 125 GPa and E_u = 2.6 GPa). (B) Reciprocal Young's modulus E^{-1} versus $\lambda^{-3/2}$ for poly(ethylene terephthalate). (C) Maximum axial Young's modulus achievable through tensile drawing as a function of molecular weight, calculated for poly(ethylene terephthalate) with eqs 1 and 3 (broken curve) and 3′ (solid line). Experimental data points were taken from the following: Pinnock and Ward,[13] "pin-only" fibers (□), "pin-and-plate" fibers (○); Pereira and Porter,[14] initial crystallinity 0% (■), 30% (●), 50% (+); Hofmann et al.,[22] M_w (▲), M_n (△).

The reported modulus/draw ratio data are presented in Figure 1A. These experimental results reveal surprisingly little variation or scatter, despite the fact that they were obtained with widely different techniques, sam-

ples, initial morphologies, etc. It is of major importance to note that the initial crystallinity (0–50%) of the isotropic samples of Pereira and Porter[14] barely effected the development of the Young's modulus with draw ratio. This finding, of course, justifies the exclusion of morphological information and details about crystallinity in the derivation of the presently employed theory[1] (see also the Discussion).

The theoretical axial modulus of PET is not a subject of harmony among the various workers. Estimates of the values of E_h range from 76 to 146 GPa.[15-21] Therefore, the data in Figure 1A were used to calculate the theoretical modulus with the aid of eq 2. Figure 1B displays a plot of E^{-1} vs $\lambda^{-3/2}$. From the intercept at $\lambda^{-3/2} = 0$, $E_h = 125$ GPa was obtained, and from the slope $E_u = 2.6$ GPa was computed. Despite scatter of the data expected at relatively low draw ratios, the calculated axial modulus shows gratifying accord with the theoretical modulus determined by a number of other authors.[16,20,21]

The development of the axial Young's modulus with draw ratio, calculated with eq 1, and with $E_h = 125$ GPa and $E_u = 2.6$ GPa, is represented by the solid line in Figure 1A. Evidently, excellent agreement is found with the experimental data.

The maximum modulus *achievable through tensile drawing* was calculated as a function the chain length with the above values of E_h and E_u and with relations 1 and 3 (broken curve) and 3′ (solid line). The results are plotted in Figure 1C. Also in this figure is indicated the maximum experimental modulus, recently reported by Hofmann et al.,[22] for a PET sample with $M_w = 20\,000$ and $M_n = 15\,000$.

It is of importance to note that most commercial-grade PETs have molecular weights in the range of 30–50 $\times 10^3$, which set a predicted upper limit around 50 GPa to the Young's modulus that can be achieved in tensile drawing.

Poly(oxymethylene). The experimental data of the room-temperature Young's modulus versus the draw ratio of oriented poly(oxymethylene) (POM), published by Clark and Scott[23] ("super-drawing"), Coates and Ward[24] (hydrostatic extrusion), and Konaka et al.[25] (microwave heating-drawing), are reproduced in Figure 2B.

Remarkably, reported experimental and theoretical estimates of the axial modulus of POM range from 40 to 220 GPa.[26-36] Therefore, the value of E_h was again derived from a plot of E^{-1} vs $\lambda^{-3/2}$ (Figure 2A). A straight line was obtained for high draw ratios, yielding a theoretical modulus of 100 GPa. From the slope E_u was calculated to be 1.6 GPa. The calculated dependence of the axial Young's modulus on the draw ratio is displayed in Figure 2B (solid line). This figure shows the remarkable agreement between the experimental data and the calculations.

Figure 2C presents the molecular weight dependence of the maximum modulus of POM calculated as before with eq 1 and both eqs 3 and 3′. The reported values of the maximum experimental Young's moduli are plotted in this graph against the values of M_n and M_w of the samples used by the various workers.

Isotactic Polypropylene. Figure 3A collects various experimental data of the Young's modulus versus the draw ratio of isotactic polypropylene (i-PP). Once more, a unique relation is observed between the modulus and draw ratio, regardless of the widely diverse preparation techniques and materials employed by the different authors. Cansfield et al.[37] and Wills et al.[38] used compression-molded sheets, Taylor and Clark[39] melt-spun fibers, and

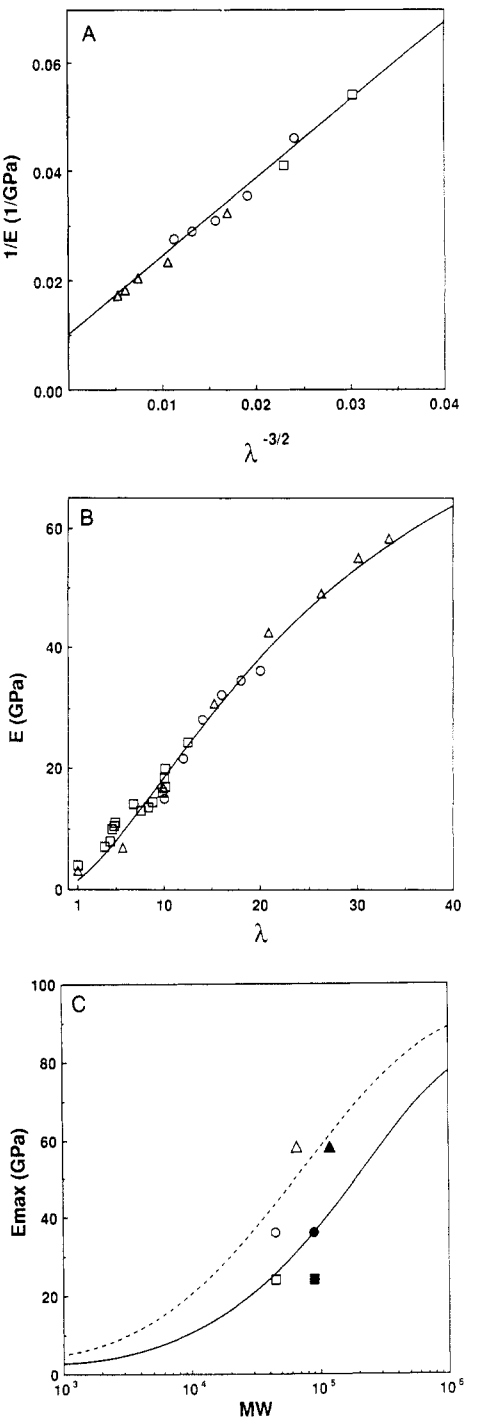

Figure 2. (A) Reciprocal Young's modulus E^{-1} versus $\lambda^{-3/2}$ for poly(oxymethylene). (B) Axial Young's modulus E versus draw ratio λ computed for poly(oxymethylene) with eq 1 (E_h = 100 GPa and E_u = 1.6 GPa). (C) Maximum axial Young's modulus achievable through tensile drawing as a function of molecular weight, calculated for poly(oxymethylene) with eqs 1 and 3 (broken curve) and 3′ (solid line): M_n, open points; M_w, closed points. Experimental data points were taken from the following: Clark and Scott,[23] (○) M_w 9 × 10⁴; Coates and Ward,[24] (□) M_w 9 × 10⁴; Konaka et al.,[25] (△) M_w 12 × 10⁴.

Peguy and Manley[40] dried gels in their respective drawing experiments.

Values of the theoretical Young's modulus reported for i-PP are between 41 and 88 GPa.[15,41] No satisfactory description of the above experimental data was obtained with either one of these extreme values. E_u and E_h were derived from the familiar E^{-1} vs $\lambda^{-3/2}$ plot (Figure 3B), yielding the respective values of 60 and 0.6 GPa. The solid line in Figure 3A represents the modulus/draw ratio

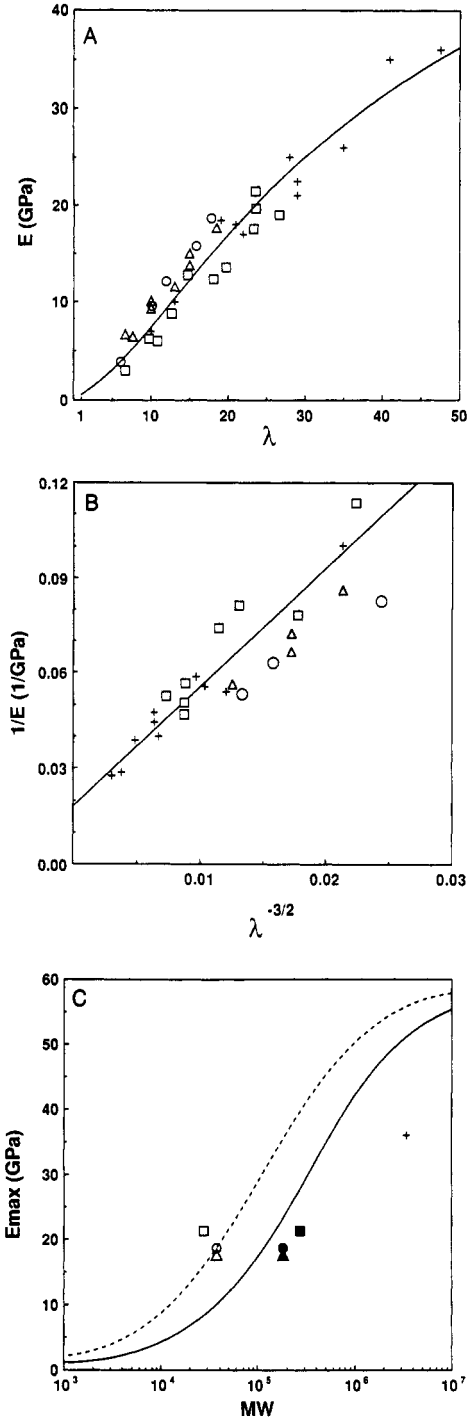

Figure 3. (A) Axial Young's modulus E versus draw ratio λ computed for isotactic polypropylene with eq 1 (E_h = 60 GPa and E_u = 0.6 GPa). (B) Reciprocal Young's modulus E^{-1} versus $\lambda^{-3/2}$ for isotactic polypropylene. (C) Maximum axial Young's modulus achievable through tensile drawing as a function of molecular weight, calculated for isotactic polypropylene with eqs 1 and 3 (broken curve) and 3′ (solid line): M_n, open points; M_w, closed points. Experimental data points were taken from the following: Cansfield et al.,[37] (○) M_w 1.81 × 10⁵; Wills et al.,[38] (△) M_w 1.81 × 10⁵; Taylor and Clark,[39] (□) M_w 2.77 × 10⁵; Peguy and Manley[40] (+) M_w 3.4 × 10⁶.

dependence calculated with these constants.

The molecular weight dependence of the maximum achievable modulus was computed with relations 1 and 3 and 3′ (see Figure 3C).

Poly(*p*-xylylene). Recently, Van der Werff and Pennings[42] prepared high-modulus fibers of poly(*p*-xylylene) (PPX) by drawing as-polymerized films at a temperature of 420 °C. Figure 4A shows their Young's

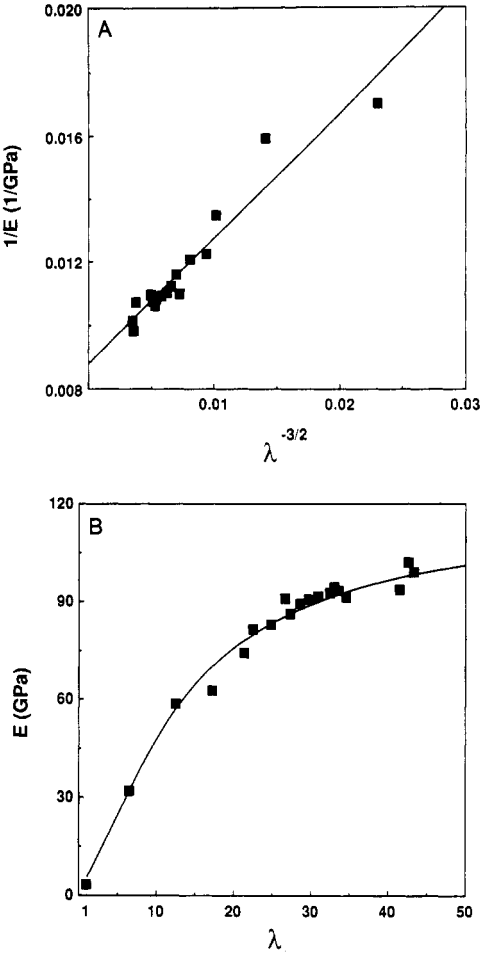

Figure 4. (A) Reciprocal Young's modulus E^{-1} versus $\lambda^{-3/2}$ for poly(*p*-xylylene). (B) Axial Young's modulus E versus draw ratio λ computed for poly(*p*-xylylene) (eq 1) with E_h = 114 GPa and E_u = 5.6 GPa. Experimental data points were taken from ref 42.

modulus/draw ratio data. Figure 4B displays the $1/E$ vs $\lambda^{-3/2}$ relationship calculated from these results. From this plot theoretical axial moduli E_h of 114 GPa and E_u of 5.6 GPa were derived. The solid curve in Figure 4A represents the calculated modulus/draw ratio dependence, which is in excellent accord with the experimental results.

Discussion

In this paper we presented the application to a number of flexible-chain polymers of a (previously introduced) simple, two-state theory for the development of the axial Young's modulus with draw ratio. Clearly, characterization of drawn polymers by only two types of elastic elements is an oversimplified representation of their actual structure. However, the outstanding agreement between calculated and experimental stiffness indicates that the complex changes in morphology and molecular structure that occur during tensile drawing are adequately reflected in the simple helix–coil representation. The excellent description of the experimental results also suggests that the stiffness of tensile-oriented polymers is controlled by factors relating to segmental orientation, on which the present theory is based, and not to the commonly measured morphological quantities such as crystallinity, crystal size, etc., that feature in a variety of other theories.

In the following section we will critically review the importance and the values of the two elastic constants,

Table II
Calculated Values of the Theoretical Axial Modulus, E_h, and the Modulus of the Unoriented Polymer, E_u (Equations 1 and 2)

polymer	E_h, GPa	E_u, GPa
poly(ethylene terephthalate)	125	2.6
poly(oxymethylene)	100	1.6
isotactic polypropylene	60	0.6
poly(*p*-xylylene)	114	5.6
polyethylene[1]	300	1.6

E_h and E_u, in the theory. The numerical values of these quantities are collected in Table II for the various polymers analyzed in this work, together with those of polyethylene (from ref 1).

***E*h.** E_h designates the stiffness of the "helical" elements, i.e., of those structural units that are perfectly oriented along the fiber axis. In this work, E_h was derived from experimental data employing relation 2. As noted above, the values of E_h are in accord with chain moduli determined by means of spectroscopic techniques, which provides confidence in our E^{-1} vs $\lambda^{-3/2}$ extrapolation procedure. Two comments are in order, however. First, it should be noted that the value of E_h is calculated from the stiffness of drawn specimens. Therefore, this value relates to the modulus of the chains in the crystal packing adopted in the tensile-drawing experiment, which not necessarily is the crystal modification of the maximum modulus (see, e.g., nylon 6[43]). Second, the theory is based on the assumption that tensile deformation proceeded in the affine mode. Experimental conditions resulting in reduced efficiency of the drawing process, such as too high temperatures, cause a decrease of the slope of the E/λ curve, and the extrapolation procedure invariably yields too low predictions of the maximum modulus E_h. This erroneous computation is readily avoided if the "molecular" draw ratio of the specimens is determined (e.g., by thermal shrinkage measurements) and employed in the calculations.

An illustrative case in point may be the results obtained for poly(*p*-xylylene). The calculated theoretical modulus of PPX (114 GPa) appears to be unexpectedly low. A potential cause for this result may be found in the disorder in the crystal lattice of the drawn PPX samples. It is known that during annealing or drawing the crystal structure of PPX transforms irreversibly into conformationally disordered β_1 (at 231 °C) and β_2 (287 °C) crystal phases.[44-47] In these structures lattice distortions are introduced due to rotational and translational motions of chains, especially in the β_2 form,[44] resulting in a reduced axial modulus. An alternative, or additional, cause for the low calculated value of E_h may be found in the very high deformation temperature adopted by Van der Werff and Pennings (420 °C; melting temperature range is 400–435 °C[45]), which may have resulted in nonaffine deformation.

***E*u.** In our two-state model, E_u represents the modulus of those structural elements, in this paper designated "coil" elements, that have *any* orientation other than along the draw axis. The coil elements may exhibit a wide range of orientations, depending on the draw ratio, and may include both nonaligned crystalline units and nonoriented segments that traditionally are considered to be amorphous. In a rigorous treatment, the different values of the stiffness associated with the various segment orientations and degrees of crystallinity all should be taken into account in the calculation of the modulus. This, of course, would be a formidable task, because of the complex nature of the coil segments; and their respective moduli are bound to depend on the draw ratio. Remarkably, the results in the present paper show that the mechanical properties of the ensemble of off-axis segments (at constant temperature and strain rate[48]) are adequately represented by only one, draw ratio independent, modulus E_u. This observation indicates that the small-strain mechanical behavior of the coil elements may be dominated by a single mode of deformation. For these nonaligned segments this mode can readily be identified as shear. Consequently, it is likely that the lowest shear modulus significantly contributes to E_u (in the present case of uniform stress). It is of interest to note that E_u for polyethylene was established to be 1.6 GPa (ref 1, Table II) and that the lower crystal shear modulus is 1.62 GPa.[48] (Unfortunately, no other crystal stiffness matrices are known in sufficient detail to expand the comparison.) The fact that E_u coincides with the shear modulus of the crystalline phase seems to indicate that the latter is the dominant modulus and that the contribution of traditional amorphous segments, which typically have much lower moduli (above the glass transition temperature), surprisingly is less important. A simple rationale for this conclusion may be that already at relatively low draw ratios the amorphous segments become highly strained and have an effective modulus that is significantly higher than that in their isotropic, nonstressed state. Interestingly, and most importantly, experimental results show that the effect of the crystallinity, or amorphous fraction, on the modulus of the undrawn, isotropic materials vanishes already at low draw ratios (see, e.g., Figure 1A), which corroborates this view.

Clearly, E_u should not be confused with the modulus, E_i, of isotropic, as-processed materials. Indeed, it is well-known that the E_i strongly depends on the degree of crystallinity. This once more is illustrated by the data of Pereira and Porter[14] for PET: the moduli of their isotropic samples range from 1.8 to 2.8 GPa for crystallinities of 0–50%. As pointed out above, however, this initial effect of the crystallinity on the modulus is relevant only at low draw ratios, where the theory is not applicable, and vanishes at draw ratios exceeding 3.

Maximum Axial Modulus. The theory clearly indicates that the theoretical stiffness E_h can only be achieved at $\lambda \rightarrow \infty$. However, as is evident from eqs 3 and 3′, the molecular weight sets an upper limit to the maximum attainable draw ratio. This implies that the highest achievable modulus of oriented materials produced through tensile deformation is ultimately dictated by the molecular weight of the polymers used. These theoretical upper limits, of course, can be approached only under conditions where other factors that could further reduce the maximum experimental draw ratio, such as chain entanglements and crystals in the case of macromolecules with strong intersegmental interactions (e.g., polyamides, etc.), are unimportant or have been removed.

As already noted in the Introduction, it is not obvious which moment of the molecular weight distribution needs to be employed in the calculation of the theoretical stiffness limits for polydisperse macromolecular systems. Clearly, deformation of a network requires a minimum number of junctions to transfer the stresses associated with the elongation of the chains. Thus, the argument can be made that an entanglement network of heterodisperse chain molecules is likely to fail when a significant fraction of the macromolecules has been extended to their full length and no longer interact through chain entanglements with other chains. This suggests that the number-averaged chain length should be substituted in relation 3, rather than M_w. It also implies that the full extension

of all macromolecules is never achieved in polydisperse polymers. Alternatively, it can be reasoned that crystallites formed during drawing may act as junction points and postpone failure of the molecular network. As a matter of fact, in some distinct cases (e.g., Figure 3C) computation with eq 3 and M_n of the maximum theoretical stiffness yields values that are below those observed experimentally. On the other hand, employing M_w and eq 3 systematically yields values that are unrealistically high. This is, of course, readily understood in the above terms of entanglement network deformation. Furthermore, previously[1] we made the observation that substitution of M_w in eq 3′ provides a fairly good description of the maximum reported experimental moduli. This trend is confirmed in the present work for some cases but certainly not for all. It is clear that the matter of the effect of polydispersity on the maximum elongation of macromolecular networks is not resolved and invites additional theoretical work. Nevertheless, at this instance, the maximum values derived from eqs 1, 2, and 3 (with M_n) and 3′ (M_w) provide useful estimates for the upper limits of the modulus that can be expected for tensile-drawn macromolecular systems of finite chain length.

Finally, it should be pointed out that the predicted maximum values of the stiffness of oriented polymers relate only to materials produced by tensile drawing. Alternative processing techniques that do not rely on tensile deformation, such as solid-state polymerization, may yield higher degress of orientations and moduli at lower molecular weights.

Acknowledgment. This work was supported by the U.S. Army Research Office. We gratefully acknowledge the help of A. Andreatta in the preparation of this manuscript and thank Prof. Dale Pearson (UCSB) for stimulating discussions on the subject of network deformation.

References and Notes

(1) Irvine, P. A.; Smith, P. *Macromolecules* **1986**, *26*, 240.
(2) Hermans, P. H. *Contributions to the Physics of Cellulose Fibres*; Elsevier: New York, 1946.
(3) Fraser, R. D. B. *J. Chem. Phys.* **1953**, *21*, 1511.
(4) Ward, I. M. *Mechanical Properties of Solid Polymers*, 2nd ed.; Wiley: New York, 1983.
(5) Bastiaansen, C. W. M.; Leblans, P. J. R.; Smith, P. *Macromolecules*, in press.
(6) Hadley, D. W.; Pinnock, P. R.; Ward, I. M. *J. Mater. Sci.* **1969**, *4*, 152.
(7) Smith, P.; Matheson, R. R., Jr.; Irvine, P. A. *Polym. Commun.* **1984**, *25*, 294.
(8) Kramer, E. J. *Adv. Polym. Sci.* **1983**, *52/53*, 33.
(9) Flory, P. J. *Statistical Mechanics of Chain Molecules*; Interscience: New York, 1969.
(10) Wallach, M. L. *Makromol. Chem.* **1976**, *103*, 19.
(11) Kokle, V.; Billmeyer, F. W. *J. Polym. Sci.* **1955**, *B3*, 47.
(12) Kinsinger, J. B.; Hughes, R. E. *J. Phys. Chem.* **1963**, *67*, 1922.
(13) Pinnock, P. R.; Ward, I. M. *Br. J. Appl. Phys.* **1964**, *15*, 1559.
(14) Pereira, J. R. C.; Porter, R. S. *J. Polym. Sci., Polym. Phys. Ed.* **1983**, *21*, 1133, 1147.
(15) Sakurada, I.; Ito, T.; Nakamae, K. *J. Polym. Sci., Part C: Polym. Symp.* **1966**, *15*, 75.
(16) Treloar, L. R. G. *Polymer* **1960**, *1*, 279.
(17) Lyons, W. J. *J. Appl. Phys.* **1958**, *29*, 1429.
(18) Dulmage, W. J.; Contois, L. E. *J. Polym. Sci.* **1958**, *28*, 275.
(19) Sakurada, I.; Ito, T.; Nakamae, K. *Makromol. Chem.* **1964**, *75*, 1.
(20) Prevorsek, D. C.; Sibilia, J. P. *J. Macromol. Sci., Phys.* **1971**, *B5*, 617.
(21) Northolt, M. G.; De Vries, H. *Angew. Makromol. Chem.* **1985**, *133*, 183.
(22) Hofmann, D.; Göschel, U.; Walenta, E.; Geiss, D.; Philipp, B. *Polymer* **1989**, *30*, 242.
(23) Clark, E. S.; Scott, L. S. *Polym. Eng. Sci.* **1974**, *14*, 682.
(24) Coates, P. D.; Ward, I. M. *J. Polym. Sci., Polym. Phys. Ed.* **1978**, *16*, 2031.
(25) Konaka, T.; Nakagawa, K.; Yamakawa, S. *Polymer* **1985**, *26*, 462.
(26) Sakurada, I.; Kaji, K. *J. Polym. Sci., Polym. Symp.* **1970**, *31*, 57.
(27) Brew, B.; Clements, J.; Davies, G. R.; Jakeways, R.; Ward, I. M. *J. Polym. Sci., Polym. Phys. Ed.* **1979**, *17*, 351.
(28) Anderson, M. R.; Harryman, M. B. M.; Steinman, D. K.; White, J. W.; Currat, R. *Polymer* **1982**, *23*, 569.
(29) Rabolt, J. F.; Fanconi, B. *J. Polym. Sci., Polym. Lett. Ed.* **1977**, *15*, 121; **1977**, *15*, 121.
(30) Sakurada, I.; Nukushina, Y.; Ito, I. *J. Polym. Sci.* **1962**, *57*, 651.
(31) Asahina, M.; Enomoto, S. *J. Polym. Sci.* **1962**, *59*, 101.
(32) Miyazawa, T. *Rep. Prog. Polym. Phys. Jpn.* **1965**, *8*, 47.
(33) Suguta, H.; Miyazawa, T. *Polym. J.* **1960**, *1*, 226.
(34) Piseri, L.; Zerbi, G. *J. Chem. Phys.* **1968**, *48*, 3561.
(35) White, J. *Structural Studies of Macromolecules by Spectroscopic Study*; Irvin, K. J., Ed.; Wiley: New York.
(36) Takeuchi, Y.; Yamamoto, F.; Nakagawa, K. *J. Polym. Sci., Polym. Lett. Ed.* **1984**, *22*, 159.
(37) Cansfield, D. L. M.; Capaccio, G.; Ward, I. M. *Polym. Eng. Sci.* **1976**, *16*, 721.
(38) Wills, A. J.; Capaccio, G.; Ward, I. M. *J. Polym. Sci., Polym. Phys. Ed.* **1980**, *18*, 493.
(39) Taylor, W. N., Jr.; Clark, E. S. *Polym. Eng. Sci.* **1978**, *18*, 518.
(40) Peguy, A.; Manley, R. St. J. *Polym. Commun.* **1984**, *25*, 39.
(41) Sakurada, I.; Kaji, K. In *Polymers and Polymerization*; Overberger, C. G., T. G. Fox, Eds.; Interscience: New York, 1970; p 57.
(42) Van der Werff, H.; Pennings, A. J. *Polym. Bull.* **1988**, *19*, 587.
(43) Kaji, K.; Sakurada, I. *J. Polym. Sci., Polym. Phys. Ed.* **1974**, *12*, 1491.
(44) Isoda, S.; Kawaguchi, A.; Katayama, K. *J. Polym. Sci., Polym. Phys. Ed.* **1984**, *22*, 669.
(45) Kirkpatrick, D. E.; Wunderlich, B. *Makromol. Chem.* **1985**, *186*, 2595.
(46) Iwamoto, R.; Wunderlich, B. *J. Polym. Sci., Polym. Phys. Ed.* **1973**, *11*, 2403.
(47) Isoda, S.; Tsuji, M.; Ohara, M.; Kawaguchi, A.; Katayama, K. *Polymer* **1983**, *24*, 1155.
(48) E_u is expected to depend on the strain rate and test temperature and account for the variation with these parameters of the modulus of drawn polymers.
(49) Tashiro, K.; Kobayashi, M.; Tadokoro, H. *Macromolecules* **1978**, *11*, 914.

Registry No. Poly(ethylene terephthalate), 25038-59-9; poly(oxymethylene), 9002-81-7; isotactic polypropylene, 25085-53-4; poly(*p*-xylylene), 25722-33-2.